doi:10.2533/chimia.2024.320 Chimia 78 (2024) 320–325

Operando X-ray Absorption Spectroscopy as a Powerful Tool for Uncovering Property-Activity Relationships for Oxygen Evolution Transition Metal Oxide Catalysts

Emiliana Fabbri*[a] and Thomas J. Schmidt[a,b]

Abstract: The development of a sustainable and environmentally friendly energy economy encompasses efficient hydrogen production from renewable energy *via* electrolysis. In this context, great efforts have recently been dedicated to the development of more efficient and cost-effective electrocatalysts. Understanding the mechanism of the oxygen evolution reaction (OER) on transition metal oxide catalysts is of great interest, but the reaction and system complexity render the characterization of active sites and the understanding of reaction mechanisms challenging. Time resolved Quick X-ray Absorption Spectroscopy (XAS) can provide dynamic snapshots of the electronic and local structure of nanocatalysts, revealing the 'real active phase' of the catalyst, which can substantially differ from the as-prepared catalyst powder or the catalyst in form of an electrode under non-operating conditions. In this contribution, several examples will be presented showing how *operando* XAS can reveal catalyst-support interactions, changes in the reaction mechanism, and dynamic reversible/irreversible changes in the electronic and local structure of OER catalysts.

Keywords: Electrocatalysts · Property/activity relationship · X-ray absorption spectroscopy · Water splitting

Emiliana Fabbri received her PhD in Materials Science from the University of Rome Tor Vergata. In 2009 she was appointed tenured scientist at the National Institute for Materials Science (NIMS), Japan. Since January 2012, she has been working at the Paul Scherrer Institute (PSI) in Switzerland on materials for electrochemical energy storage and conversion. To gain a fundamental understanding of electrochemical reaction mechanisms and catalytic activity descriptors, she is particularly interested in the surface chemistry and electronic structure of catalysts studied by *operando* X-ray synchrotron techniques. Emiliana Fabbri was awarded an SNSF PRIMA grant in 2020 and since 2024 she is co-leader of the Electrocatalysis and Interfaces group of the Electrochemistry Laboratory of PSI.

Thomas J. Schmidt received his PhD in Chemistry from Ulm University, Germany. He has spent his career at Lawrence Berkely National Laboratory and Paul Scherrer Institute as Post-Doc and Staff Scientist, before he worked for eight years in industrial fuel cell research at BASF Fuel Cell. He became Chair of Electrochemistry at ETH Zurich in 2011 combined with being Head of the Electrochemistry Laboratory at PSI. Since 2018, he is head of the PSI Energy & Environment Research Division. His research includes all aspects of electrochemical energy conversion and storage.

1. Introduction

The development of energy storage systems is necessary in order to mediate the variable nature of energy production from renewable resources in the course of the replacement of energy technologies based on fossil fuels. Water electrolyzers are central to the development of a clean, reliable, zero-emission hydrogen economy as they are electrochemical energy conversion devices capable of producing hydrogen from renewable energy sources.[1] Water electrolyzers are typically categorized on the basis of operating temperature and electrolyte type. Low temperature electrolyzers can be categorized into polymer electrolyte water electrolyzers (PEWEs), which are based on an acidic, proton conducting electrolyte polymer, and alkaline water electrolyzers (AWEs). The main advantages of PEWEs are the fast kinetics of the cathodic hydrogen evolution reaction and high voltage efficiencies at high current densities. However, under the typical operating conditions of a PEWE, only a few electrode materials can provide adequate stability. Therefore, the anodic and cathodic reactions are generally catalyzed by noble metal-based catalysts such as Pt, Ru and Ir. The main advantage of AWEs is that several materials provide adequate stability when in contact with an alkaline electrolyte. Therefore, a wide range of catalyst materials can be investigated as alternatives to noble metals. The potential replacement of noble metal catalysts with inexpensive and abundant transition metal-based oxides is one of the major advantages of AWE devices over PEWEs, as it allows for cost reductions that facilitate widespread market penetration.

The oxygen evolution reaction (OER) is central to the development of efficient water electrolysis, as this reaction, even with state-of-the-art (and expensive) materials such as IrO_2, is hindered by sluggish kinetics and substantial overpotential losses in both

*Correspondence: Dr. E. Fabbri, E-mail: emiliana.fabbri@psi.ch
[a]Electrochemistry Laboratory, Paul Scherrer Institute, Forschungsstrasse 111, CH-5232 Villigen PSI, Switzerland; [b]Institute for Molecular Physical Sciences, ETH Zurich, CH-8093 Zurich, Switzerland

acid and alkaline conditions.[2] The development of cost-effective, robust and highly active anode materials for OER is therefore a major challenge and has been the focus of much research attention. To this end, significant R&D efforts have been devoted to screening the OER activity and stability of various candidate materials. State-of-the-art anodic electrodes for PEWEs and AWEs are based on IrO_2 and NiO catalysts, respectively. However, recently new classes of promising electrocatalysts for OER have emerged, such as CoO_x, perovskite oxides with an ABO_3 structure[3] or MOF-based[4] catalysts.

Understanding the mechanism of the oxygen evolution reaction (OER) on transition metal oxide catalysts for application in alkaline electrolyzers is of great interest, but the complexity of the reaction and the system makes the understanding of the reaction mechanism challenging. In fact, it has recently been recognized that the OER may also involve the oxidation of lattice oxygen and significant reconstruction of the catalyst surface.[2] Fig. 1 shows a sketch of an OER reaction mechanism involving oxidation of lattice oxygen to produce oxygen molecules (*i.e.* the lattice oxygen evolution reaction, LOER) and dissolution of the catalyst cation for a perovskite ABO_3 catalyst, leading to surface reconstruction with formation of an oxyhydroxide layer.[3] The process of transition metal oxide surface reconstruction during OER has been demonstrated previously by our group using Quick X-ray Absorption Spectroscopy under real operating conditions.[5] Time-resolved Quick-XAS can provide dynamic snapshots of the electronic and local structure of nanocatalysts, revealing the 'real active phase' of the catalyst, which may differ significantly from the as-prepared catalyst powder or the catalyst in the form of an electrode under non-operating conditions. Our quick *operando* XAS investigations on different transition metal oxide OER catalysts have shown that the most active catalysts are prone to change during the electrochemical reaction;[5] therefore, besides performing *ex situ* characterizations, the ability to obtain dynamic snapshots of the physico-chemical properties of the catalyst under operating conditions becomes central for a proper understanding of the OER mechanism.[6] In particular, we were able to show that the key to highly active catalysts is a self-assembled (oxy)hydroxide surface layer.[5] This new concept completely revolutionizes the currently most accepted view of the design principles for highly active perovskite OER catalysts and points to the paramount need for in-depth study of the surface properties of perovskite catalysts under *operando* conditions.

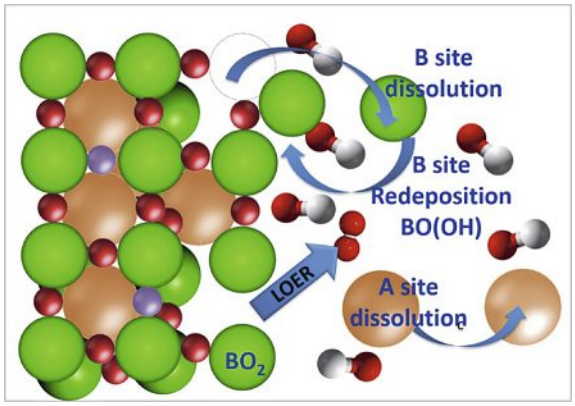

Fig. 1. Sketch showing LOER and cation dissolution at the surface of an ABO_3 perovskite oxide catalyst. The A- and B-site cations dissolved from the perovskite surface because of LOER and/or chemical dissolution may be further dissolved in the electrolyte or redeposited on the perovskite surface, ultimately forming an oxyhydroxide layer. Figure reprinted with permission from ref. [3].

The previous example highlights the importance of performing *operando* XAS measurements (*i.e.* under operating conditions when the reaction of interest is occurring, and catalyst activity can be measured) to understand the true active phase of a transition metal oxide catalyst during OER and thus formulate meaningful property/activity relationships. The first step in achieving a reliable *operando* XAS electrochemical experiment is the design of a spectro-electrochemical cell. The cell design is fundamental to perform reliable electrochemical measurements while optimizing the XAS signal. For our group's *operando* Quick-XAS measurements, a spectro-electrochemical flow cell has been designed as shown in Fig. 2.[7] The cell is composed of three parts: The main electrochemical compartment is formed by the central hole in the middle part, which was confined by two gold-coated Kapton foils, which served as windows for the X-ray beam. The lower Kapton foil could be used as a substrate for the working electrode and the upper Kapton foil as a counter electrode. A second electrolyte compartment, located downstream of the main central compartment along the electrolyte channel, allowed the insertion of a reference electrode.

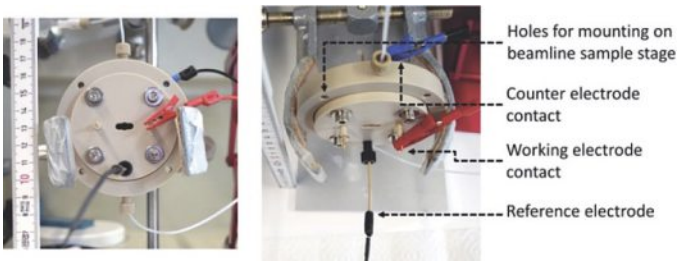

Fig. 2. Pictures of the spectro-electrochemical flow cell from Binninger *et al.* Scale in cm. Figure reprinted with permission from ref. [7].

2. NiO and CoO_x-based OER Catalysts

Ni-based oxides are among the most promising OER catalysts in alkaline electrolytes due to the abundance of Ni and the satisfactory performance in terms of both activity and stability. The OER activity of NiO can be enhanced by adding Fe into the rock salt structure of NiO or by absorbing Fe from the electrolyte, and in recent years many studies have been directed toward understanding the distinct role of Fe in the OER mechanism and activity. A recent review of studies dealing with reversible and irreversible transitions of NiO-based catalysts during OER and the correlation of these transitions with their OER activity has been published by our group.[8]

To study Ni-based OER catalysts, we have employed a scalable synthesis method, the flame spray synthesis, capable of producing large batches of crystalline Ni-Fe oxide nanoparticles with high specific surface areas in the range of 20-75 m^2g^{-1}.[9] The (high resolution) transmission electron microscopy (HR-)TEM images of the NiO, $Ni_{0.9}Fe_{0.1}O$ and $Ni_{0.7}Fe_{0.3}O$ samples are shown in Fig. 3.[9] By performing *operando* XAS measurements on these samples, XANES and EXAFS analyses at the Ni and Fe K-edges allow us to extract useful information about changes in valence states and local structure of the catalysts during OER.[9] In particular, the *operando* XAS data suggests that the incorporation of Fe stabilizes the electronic and local coordination environment of Ni under OER operating conditions, inhibiting the transformation to a more layered and disordered (oxy)hydroxide structure typical of NiO catalysts.

Cobalt oxides also exhibit good OER activity in alkaline electrolytes. The two most common cobalt oxide structures are rock salt/wustite (rs-CoO) and spinel. Also, in the case of Co-based oxides, the OER activity can be greatly enhanced by the incor-

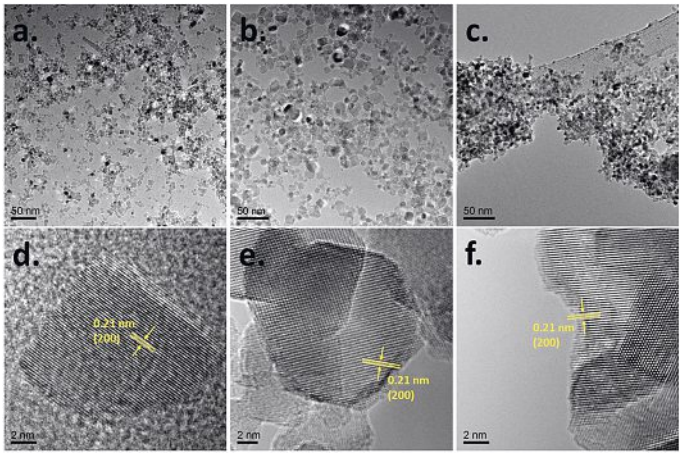

Fig. 3. High resolution TEM images of flame spray synthesized NiO (a and d) $Ni_{0.9}Fe_{0.1}O$ (b and e), and $Ni_{0.7}Fe_{0.3}O$ (c and f) nanoparticles. Figure adapted with permission from ref. [9]. Copyright **2021** *Royal Society of Chemistry*.

poration of Fe, and again, neither the optimal Fe content nor the reason for the enhanced activity is clearly understood.

Using flame spray synthesis,[10] we have synthesized $Co_{1-x}Fe_xO_y$ nanoparticles. By combining surface and bulk sensitive analysis techniques, we discovered that the sample exhibits a gradual change in structure/composition from the bulk to the catalyst surface as a function of Fe content.[11] The CoO_y sample consists of rock salt CoO in the bulk and a Co_3O_4 phase at the surface, which hinders reversible and irreversible changes of the Co oxidation state during the applied OER potential, resulting in a lower OER activity compared to Fe-containing samples with Fe content up to x = 0.4. In contrast, the samples with higher Fe content than x = 0.4 initially present a uniform $CoFe_2O_4$ structure, which decreases the mass OER current density due to a decrease in the Co active site. However, the activity normalized for the Co content still increases with the increase of the Fe content in the $Co_{1-x}Fe_xO_y$ samples. Indeed, high Fe content promotes the presence of Co in oxidation state 2+ in the octahedral site, thus boosting irreversible surface modification during OER.[11]

We have also investigated an alternative strategy to boost CoO_x OER activity, namely creating nanocomposites to exploit beneficial synergistic effects by combining CoO_x with ceria oxide. CeO_2 is known to be able to enhance the OER activity of CoO_x, even though the rational of the synergy between the two materials is not yet understood. In our study,[12] we have used *operando* hard X-ray absorption spectroscopy (hXAS) to monitor the Co K edge and Ce L3 edge in a flame spray synthesized CoO_x/CeO_2 composite to reveal the evolution of the Co and Ce oxidation states during OER. In addition, *ex situ* soft XAS (sXAS) characterization in total electron yield mode (TEY) has provided useful information on the irreversible surface-specific transformations of the Co L3 edge and of the O K edge.[12] Electrochemical characterization, coupled with *operando* h-XAS and TEY, showed that CeO_2 is not an active catalyst for the OER, but coupling CeO_2 with CoO_x introduces significant modifications in the Co and O species at the CoO_x catalyst surface modifying the flat band potential and promoting to more favorable Co oxidation state transformations during OER. Fig. 4[12] shows *operando* Quick-XAS characterizations of CoO_x and CoO_x/CeO_2 composite to monitor the *operando* evolution of Co K edge and Ce L3 edge during cycling voltammetry measurements. The ΔE_{edge}, obtained by comparing the energy of the absorption edge (E_{edge}) at the specific potential with that at 1.0 V RHE measured at the beginning of the *operando* measurements of CoO_x, overlaps in the first anodic and cathodic scan, with no obvious changes even at the end of the last tenth cyclic voltammograms. Differently, the ΔE_{edge} of CoO_x/CeO_2 composite shows an increase of ≈27 meV as the potential decreases from 1.6 to 1.0 V RHE at the end of the last tenth cyclic voltammograms, indicating a partial irreversible oxidation of Co atoms for CoO_x/CeO_2 composite. This result highlights that the reversibility of Co oxidation is slightly modified by the formation of the CoO_x/CeO_2 composite, leading to a larger extent of surface reconstruction and thus higher OER activity.[12] The periodic change of the Co K-edge as a function of the applied potential indicates that Co is the active center for OER. In comparison, the evolution of the Ce oxidation state was monitored *via* the Ce L3 edge spectra, with no apparent changes in E_{edge} for Ce L3 edge with applied potential, indicating that Ce is not redox active during OER.[12]

3. Perovskite Oxide OER Catalysts

The basic perovskite oxide structure can be represented as ABO_3, where A is the larger cation, such as a lanthanide or alkaline earth element, and B is the smaller cation, usually a transition metal. The ABO_3 structure allows for a wide range of cation substitution by partial substitution of either the A or B cation with another element, leading to an immense range of compositional possibilities. Therefore, the research is mainly focused on the identification of catalytic or activity descriptors able to predict the optimal physicochemical properties to maximize the OER activity with the aim to the rapid design of novel, highly active perovskite materials.

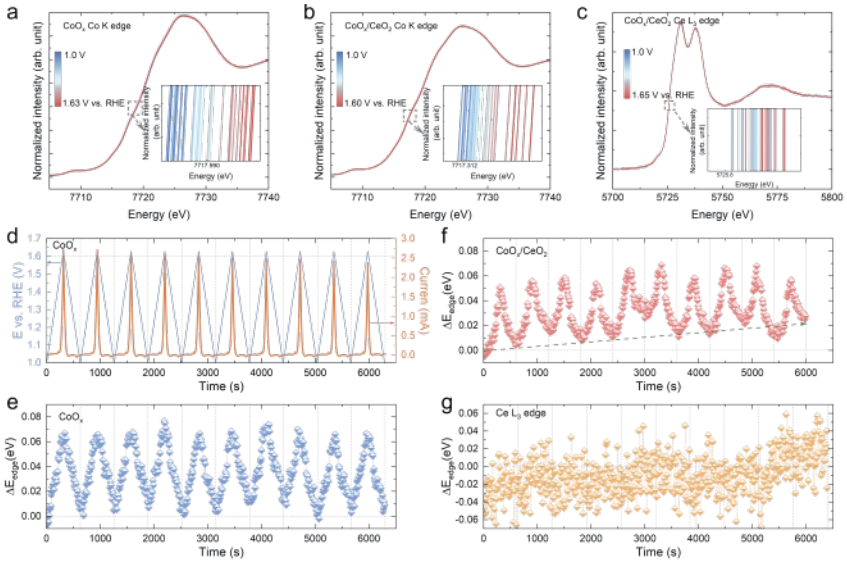

Fig. 4. XANES spectra at the a) Co K edge of CoO_x, b) Co K edge of CoO_x/CeO_2 and c) Ce L3 edge of CoO_x/CeO_2 during the first anodic cyclic voltammetry in OER potential range. Insets in panel (a–c) highlights the shift in absorption edge. d) The applied potential and the OER current of CoO_x electrode as a function of time during 10 cyclic voltammograms of the *operando* Quick-XAS characterization. The corresponding energy shift (ΔE_{edge}) at the Co K edge spectra for e) CoO_x and f) CoO_x/CeO_2 during cyclic voltammograms. g) The ΔE_{edge} at the Ce L3 edge spectra for the CoO_x/CeO_2. Figure reprinted with permission from ref. [12].

Fabbri *et al.* used *operando* Quick-XAS measurements to show that one of the most active perovskite catalysts, $Ba_{0.5}Sr_{0.5}Co_{0.8}Fe_{0.2}O_{3-d}$ (BSCF), undergoes surface reconstruction during OER, changing its electronic and local structure under operating conditions.[5] In particular, BSCF is highly prone to develop a highly active, self-assembled (Co/Fe)OOH phase on top of the perovskite structure, as shown in Fig. 5, as a result of LOER and metal dissolution processes.[5]

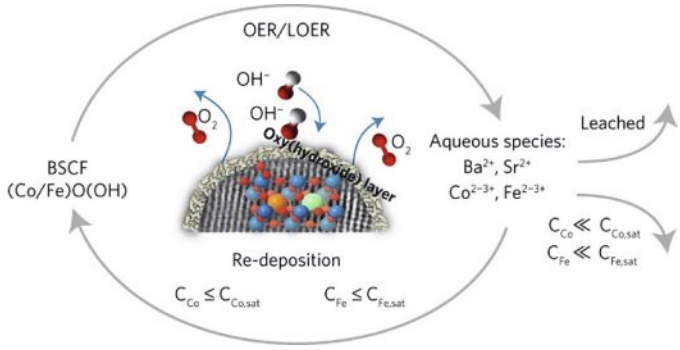

Fig. 5. sketch for the OER/LOER and cation dissolution mechanism for for BSCF catalyst leading to the formation of a Co/Fe oxyhydroxide layer. Figure adapted with permission from ref. [5]. Copyright **2017** *Nature Publishing Group*.

The great ability of BSCF to form a self-assembled, stable and highly active oxyhydroxide layer under OER conditions was attributed to the high flexibility of BSCF to accommodate the amount of oxygen vacancies. Indeed, BSCF with Co in a reduced oxidation state, and thus with a high amount of oxygen vacancies, has been shown to have higher OER activity than the same perovskite composition with Co cations in a more oxidized state (*i.e.* with higher oxygen content) or compared to CoO_x catalysts with lower oxygen vacancies.[5] Indeed, Fig. 6 shows a comparison between three OER transition metal oxide catalysts (BSCF, $La_{0.2}Sr_{0.8}CoO_3$ (LSC) and CoO_x) in terms of OER activities and changes in Co K-edge XANES and Fourier transform (FT)-EXAFS between 1.2 and 1.55 V RHE. The amount of increase in Co oxidation state and change in local atomic structure correlates with OER activity: BSCF exhibits the highest OER activity and undergoes the largest changes in both electronic and local atomic structure. The shift of the Co K-edge position decreases from ~0.7 to ~0.15 eV from BSCF to CoO_x. Furthermore, while visible changes can be observed in the BSCF FT-EXAFS, the *operando* FT-EXAFS of CoO_x is largely unchanged. LSC shows intermediate electronic structure and local structure changes as well as intermediate OER activity. Therefore, the correlation between OER activity and electronic/local structure changes measured by *operando* Quick-XAS suggests that there is a correlation between OER activity and *operando* changes in electronic and geometric structure.[5]

We have also shown that doping 20% of the Co sites with Fe in BSCF catalysts allows the Co to be in a lower oxidation state, increasing the oxygen vacancies and maximizing the OER activity.[13] *Operando* XANES spectra show an exponential increase in the shift of the Co K-edge position in the OER potential region, which is more pronounced for the BSCF compared to the $Ba_{0.5}Sr_{0.5}CoO_{3-d}$ perovskite (BSC, no Fe doping). Furthermore, Fig. 7[13] shows the *operando* FT-EXAFS spectra of BSC and BSCF in the OER regime. A growth of the coordination peak at 2.8 Å associated with the Co-Co coordination shell of Co-O(OH) is observed for both catalysts during OER. BSCF shows a larger growth of this contribution compared to BSC, indicating a more

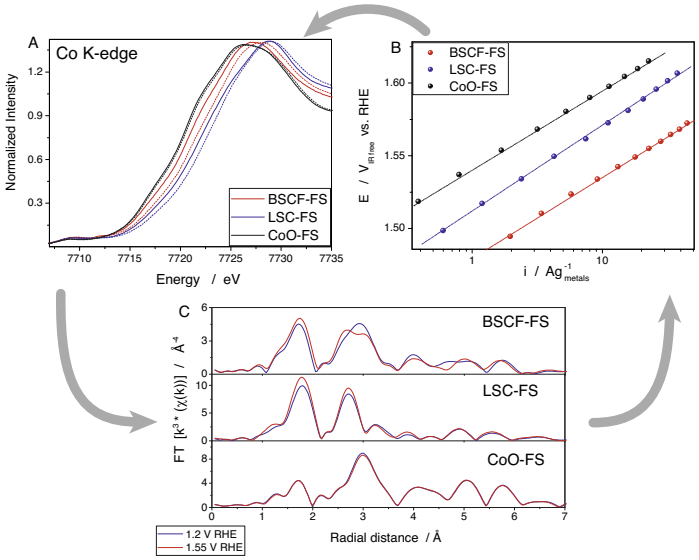

Fig. 6. a) XANES spectra recorded at the Co K-edge of BSCF, LSC and CoO electrodes at 1.2 to 1.55 V RHE in 0.1 M KOH. b) Comparison of the Tafel plots obtained by chronoamperometric measurements in 0.1 M KOH for BSCF, LSC and CoO catalysts. c) Fourier-transform (FT) of the k^3-weighted EXAFS recorded for BSCF, LSC and CoO catalysts at the applied potentials of 1.2 and 1.55 V RHE in 0.1 M KOH. Figure adapted with permission from ref. [5]. Copyright **2017** *Nature Publishing Group*.

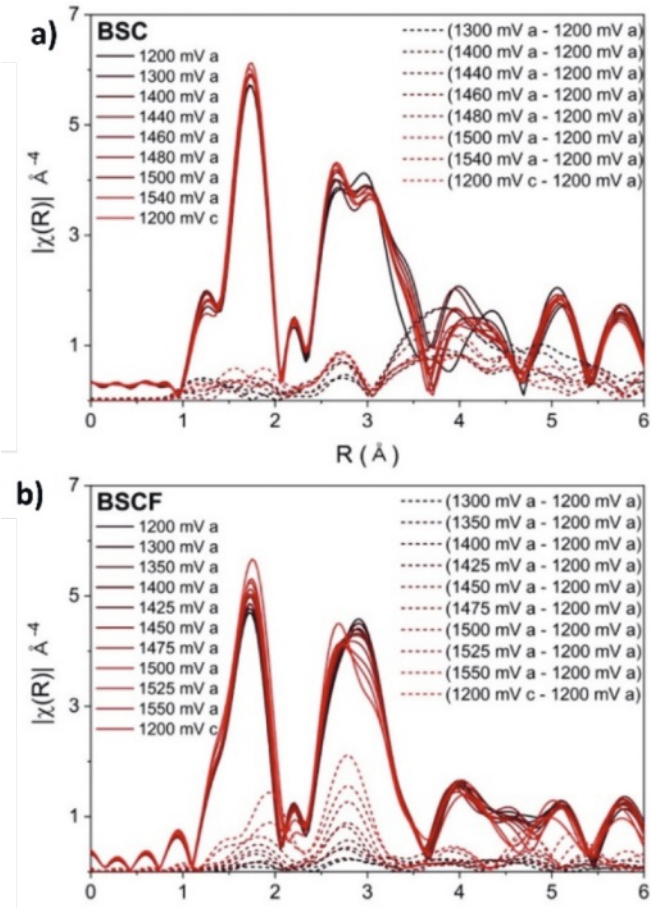

Fig. 7. Fourier transformed (FT) k^3-weighted Co K-edge EXAFS spectra of a) BSC and b) BSCF recorded during the *operando* XAS measurement (—). FT difference spectra between individual spectrum and the spectrum recorded at 1.20 V_{RHE} of the anodic polarization (---). Figure adapted with permission from ref. [13]. Copyright **2019** *American Chemical Society*.

extensive growth of a self-assembled Co-Oxy(hydroxide) layer resulting from the LOER/OER processes. Combining all the data presented in ref. [13], it can be suggested that the presence of Fe allows the incorporation of Co atoms into the perovskite structure in a lower oxidation state without the formation of secondary phases. The secondary phases can hinder the formation of the active self-assembled oxy(hydroxide) layer, resulting in lower OER activity. Overall, the maximum development of a self-assembled oxy(hydroxide) layer is required to achieve a high OER activity, as is the case for BSCF.[13]

Recently, the effect of Fe-content on the surface reconstruction of flame-spray synthesized $Ba_{0.5}Sr_{0.5}Co_{1-x}Fe_xO_{3-\delta}$ ($BSCo_{1-x}Fe_x$) series has been investigated more systematically by gradually replacing Co with Fe ($0 < x < 1$).[14] The electrochemical characterization showed a volcano-shaped trend of the OER activity as a function of Fe content, indicating $BaSrCo_{0.8}Fe_{0.2}$ as the best performing electrocatalyst. *Operando* XAS measurements revealed that the trend of OER activity with Fe-content is directly correlated with the extent of surface reconstruction that occurs under OER conditions. More specifically, the increasing OER activity for the $BSCo_{1-x}Fe_x$ from $x = 0$ to 0.2 is explained by the ability of Fe to stabilize surface Co^{2+} ions in the pristine material, which triggered irreversible surface Co oxidation and more extensive formation of a Co- and Fe-based (oxyhydr)oxide layer. The decreasing OER activity for $BSCo_{1-x}Fe_x$ with $x > 0.2$ is related to the increasing oxygen content in the pristine material, which leads to a stabilization of the bulk structure and prevents the formation of the (oxyhydr)oxide active layer, similar as it was observed for Fe doped NiO catalysts.[9] Moreover, a high Fe content ($x > 0.4$) further stabilizes the surface Co^{2+} atoms to such an extent that the irreversible surface Co oxidation is almost completely suppressed, limiting the reconstruction process and thus hindering the OER activity.[14]

In addition to doping, we have also investigated possible catalyst/support interactions in the case of BSCF. Carbon is often used as a conductive additive in the catalyst layer to increase conductivity. However, the effect of carbon addition to perovskites on electrochemical activity is often not discussed and not well understood. In a recent work,[15] composites of BSCF and conductive additives, carbon and indium-doped tin oxide, are compared.

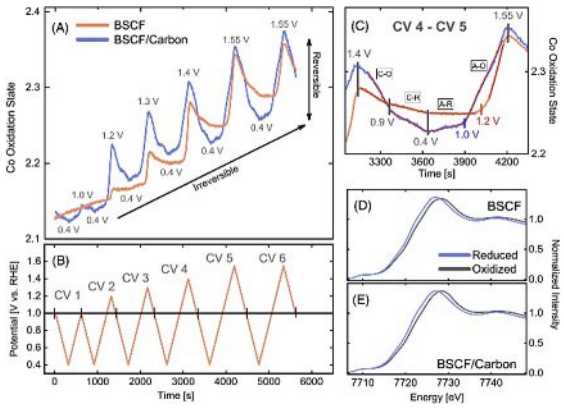

Fig. 8. a) Changes in Co oxidation state over time measured by *operando* XAS as the potential is cycled between reducing and oxidizing potentials. b) The applied potential over time during 6 cyclic voltammograms. c) Zoom in the region between cyclic voltammogram 4 and 5, which highlights the different linear fit slopes that occur in different potential ranges. d, e) XAS spectra of the most reduced and oxidized states that occur during the 6th cyclic voltammogram. Figure adapted with permission from ref. [15].

The study shows that different conductive additives have different effects on OER (and also oxygen reduction reaction, ORR) activity and cobalt redox behavior, with carbon being the additive that shows the more pronounced catalyst/support interaction. To further elucidate these differences between BSCF and BSCF/carbon, *operando* XAS measurements were performed simultaneously with cyclic voltammetry in the ORR and OER regions and the continuous changes in Co oxidation state are observed with high time resolution of 2 mV per spectrum as shown in Fig. 8. Based on our results, we suggest that carbon enhances the redox activity of Co and as a result, the oxygen electrocatalytic activities are also enhanced.[15]

In another study,[16] we have investigated the perovskite OER activity in electrolytes with different pH's and from the changes in the perovskite structure during the OER process, certain aspects regarding the reaction mechanism could be interestingly elucidated. Differences in OER activity and reaction order between alkaline and near-neutral pH regions suggest that different reaction mechanisms predominate in the different pH regions (Fig. 9).[16,17] By monitoring the changes in the energy position of the Co-K absorption edge during OER, the potential-induced increase in Co oxidation state was found only at alkaline pH (*i.e.* pH 13) for BSC and BSCF. Combined with the results of *operando* FT-EXAFS spectra, this increase of Co oxidation state was related to the development of Co/Fe-oxy(hydroxide) surface layer, which, as explained before, is related to the LOER mechanism. In contrast, in the near neutral region, the development of a Co/Fe-oxy(hydroxide) surface layer was not clearly observed by *operando* XAS.[16]

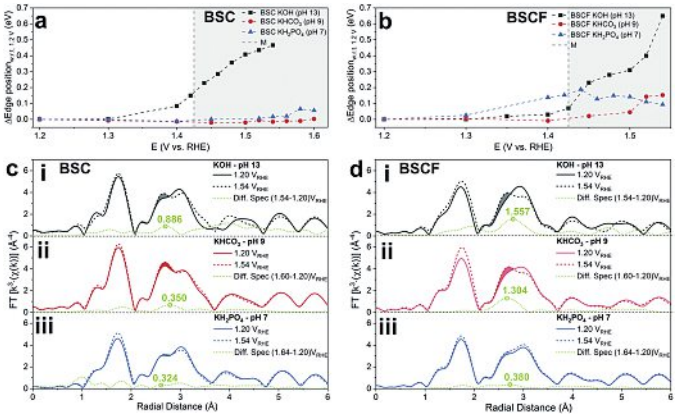

Fig. 9. The Co K-edge shift measured with respect to the edge position at 1.2 V_{RHE} at each potential during operando XAS at pH 7, 9, and 13 for a) BSC and b) BSCF. FT-EXAFS spectra recorded at 1.2 and 1.54 V_{RHE} for c) BSC and d) BSCF at (i) pH 13, (ii) pH 9, and (iii) pH 7. Figure adapted with permission from ref. [16]. Copyright **2021** *Royal Society of Chemistry*.

The investigation of perovskite OER activity and electronic and local structure changes by *operando* XAS in a wide electrolyte pH range[16] suggest that the LOER is the predominant reaction mechanism in alkaline condition, while the concerted proton-electron mechanism (the classical oxygen evolution mechanism) is more favorable at quasi-neutral pH. Nevertheless, a catalyst would not perform oxygen evolution by only one of the two mechanisms discussed here but uses rather preferentially and proportionally both paths of plausible mechanisms.

4. Conclusions

Transition metal oxide OER catalysts are a complex system to study because a single property change also modifies the elec-

tronic configuration, local and crystal structure, oxygen content, and conductivity. These are all properties that must be taken into account when considering OER activity versus a single perovskite property. Unfortunately, this makes it very difficult to identify activity descriptors and understand the specific reaction mechanism occurring at the OER catalyst surface.

Operando XAS is a powerful tool in electrochemistry to simultaneously monitor electronic and local structure changes of transition metal oxide catalysts during the OER process. We have shown that *operando* XAS measurements have revealed for different types of OER catalysts the 'real active surface' for OER, which is almost always different from the surface of the pristine catalyst or the catalyst under *non operando* conditions. In addition, by showing the behavior of different catalysts under operating conditions, *operando* XAS allows the formulation of design principles for highly active OER catalysts. The main drawback is that using hard X-rays the whole catalyst bulk is probed, while only the surface is involved in the OER process. This requires the use of small nanoparticle samples, which are difficult to obtain for many materials.

Acknowledgements

E.F. gratefully acknowledge the Swiss National Science Foundation through its PRIMA grant (grant no. PR00P2_193111). TJS thanks the Swiss Center of Excellence for NetZero Emissions.

Received: March 22, 2024

[1] E. Fabbri, A. Habereder, K. Waltar, R. Kotz, T. J. Schmidt, *Catal. Sci. Technol.* **2014**, *4*, 3800, https://doi.org/10.1039/C4CY00669K.
[2] E. Fabbri, T. J. Schmidt, *ACS Catalysis* **2018**, *8*, 9765, https://doi.org/10.1021/acscatal.8b02712.
[3] C. E. Beall, E. Fabbri, T. J. Schmidt, *ACS Catalysis* **2021**, *11*, 3094, https://doi.org/ 10.1021/acscatal.0c04473.
[4] J. Linke, T. Rohrbach, M. Ranocchiari, T. J. Schmidt, E. Fabbri, *Curr. Opin. Electrochem.* **2021**, *30*, 100845, https://doi.org/10.1016/j.coelec.2021.100845
[5] E. Fabbri, M. Nachtegaal, X. Cheng, T. Binninger, B. Kim, J. Durst, F. Bozza, T. Graule, N. Danilocic, K. E. Ayers, T. J. Schmidt, *Nat. Mater*. **2017**, *16*, 925, https://doi.org/10.1038/nmat4938.
[6] E. Fabbri, D. F. Abbott, M. Nachtegaal, T. J. Schmidt, *Curr. Opin. Electrochem*. **2017**, *5*, 20, https://doi.org/10.1016/j.coelec.2017.08.009.
[7] T. Binninger, E. Fabbri, A. Patru, M. Garganourakis, J. Han, D. F. Abbott, O. Sereda, R. Kotz, A. Menzel, M. Nachtegaal, T. J. Schmidt, *J. Electrochem. Soc.* **2016**, *163*, H906, https://doi.org/10.1149/2.0201610jes.
[8] N. Hales, T. J. Schmidt, E. Fabbri, *Curr. Opin. Electrochem*. **2023**, *38*, 101231, https://doi.org/10.1016/j.coelec.2023.101231.
[9] D. F. Abbott, E. Fabbri, M. Borlaf, F. Bozza, R. Schäublin, M. Nachtegaal, T. Graule, T. J. Schmidt, *J. Mat. Chem. A* **2018**, *6*, 24534, https://doi.org/10.1039/C8TA09336A.
[10] D. Aegerter, M. Borlaf, E. Fabbri, A. H. Clark, M. Nachtegaal, T. Graule, T. J. Schmidt, *Catalysts* **2019**, *11*, 38, 34787, https://doi.org/10.1021/acsami.9b04456.
[11] D. Aegerter, E. Fabbri, N. S. Yüzbasi, N. Diklić, A. H. Clark, M. Nachtegaal, C. Piamonteze, J. Dreiser, T. Huthwelker, T. Graule, T. J. Schmidt, *ACS Catalysis* **2023**, *13*, 15899, https://doi.org/10.1021/acscatal.3c04138.
[12] J. Huang, N. Hales, A. H. Clark, N. S. Yüzbasi, C. N. Borca, T. Huthwelker, T. J. Schmidt, E. Fabbri, *Adv. Energy Mater*. **2024**, *14*, 2303529, https://doi.org/10.1002/aenm.202303529.
[13] B.-J. Kim, E. Fabbri, D. F. Abbott, X. Cheng, A. H. Clark, M. Nachtegaal, M. Borlaf, I. E. Castelli, T. Graule, T. J. Schmidt, *J. Am. Chem. Soc*. **2019**, *141*, 5231, https://doi.org/10.1021/jacs.8b12101.
[14] D. Aegerter, E. Fabbri, M. Borlaf, N. S. Yüzbasi, N. Diklić, A. H. Clark, V. Romankov, C. Piamonteze, J. Dreiser, T. Huthwelker, T. Graule, T. J. Schmidt, *J. Mater. Chem. A* **2024**, *12*, 5156, https://doi.org/10.1039/D3TA06156F.
[15] C. E. Beall, E. Fabbri, A. H. Clark, N. S. Yüzbasi, T. Graule, T. J. Schmidt, *EcoMat* **2023**, *5*, e12353, https://doi.org/10.1002/eom2.12353.
[16] B.-J. Kim, E. Fabbri, M. Borlaf, D. F. Abbott, I. E. Castelli, M. Nachtegaal, T. Graule, T. J. Schmidt, *Mater. Adv.* **2021**, *2*, 345, https://doi.org/10.1039/D0MA00661K.
[17] W. Yoshimune, J. B. Falqueto, A. H. Clark, N. S. Yüzbasi, T. Graule, D. Baster, M. El Kazzi, T. J. Schmidt, E. Fabbri, *Small Structures* **2023**, *4*, 2300106, https://doi.org/10.1002/sstr.202300106.